4-Methylcatechol-treated Jute-Bamboo Hybrid Composites: Effects of pH on Thermo-Mechanical and Morphological Properties

Fui Kiew Liew,[a,c,*] Sinin Hamdan,[a] Md Rezaur Rahman,[b] Mohamad Rusop Mahmood,[d] Md. Mizanur Rahman,[a] Josephine Chang Hui Lai,[b] and Md. Tipu Sultan [b]

Hybrid composites were fabricated with 4-methylcatechol-treated jute and bamboo fiber at different pH levels. The effects of different pH levels on the thermal, mechanical, and morphological properties of jute-bamboo hybrid composites were investigated. Fabricated hybrid composites were characterized by Fourier transform infrared spectroscopy (FTIR), thermogravimetric analysis (TGA), differential scanning calorimetry (DSC), dynamic mechanical thermal analysis (DMTA), and adhesion test analysis. Additionally, surface morphology and tensile testing were reported. Fourier transform infrared spectroscopy (FTIR) revealed that the peak intensities at 1634 and 1643 cm^{-1} disappeared in treated jute and bamboo fibers. This resulted from the removal of hydroxyl groups on the treated fibers. A higher pH (9 or 10) resulted in the effective modification of bamboo and jute fibers. The TGA results showed that the presence of hybrid fiber led to an earlier degradation of the hybrid composite. The DSC results showed that the crystallinity index declined by 7% to 8%, which improved the adhesion between the fiber and the polymer. According to these finding, the pH level contributed to an improvement in the mechanical properties of the composites. The pH 10-treated hybrid composites exhibited the highest tensile strength and modulus. The surface morphology revealed that at higher pH, the treated hybrid composites exhibited strong adhesion characteristics.

Keywords: 4-Methylcatechol; Hybrid composite; pH; Thermo-mechanical; Morphological

*Contact information: a: Department of Mechanical and Manufacturing Engineering, Faculty of Engineering, University Malaysia Sarawak, 94300 Kota Samarahan, Sarawak, Malaysia; b: Department of Chemical Engineering and Energy Sustainability, Faculty of Engineering, University Malaysia Sarawak, 94300 Kota Samarahan, Sarawak, Malaysia; c: Faculty of Applied Science, Universiti Teknologi Mara, Kota Samarahan, Sarawak, Malaysia; d: Nano-SciTech Centre (NST), Institute of Science, Universiti Teknologi Mara, 40450 Shah Alam, Selangor, Malaysia; *Corresponding author: liewsan2004@gmail.com*

INTRODUCTION

In recent years, research involving natural fibers composites has been performed. Plant-based natural fibers act as the reinforcing material for composites (Botelho *et al*. 2006; Lee *et al*. 2008; Takagi 2010; Kim and Ye 2012). These fibers have high strength and stiffness, combined with low cost, light weight, renewable, and biodegradable (Nunna *et al*. 2012; Hitoshi *et al*. 2014; Rahman *et al*. 2015). The future of natural fiber composites appears to be promising, with many advantages over glass fiber composites (Joshi *et al*. 2004).

Jute is an agro-based monocotyledon, commonly grown in India, China, and Bangladesh. Currently, jute and jute-based materials contribute less than 5% of Bangladesh's total exports (Jahan *et al*. 2009). The availability of a large quantity of low

cost jute fiber with well-defined mechanical properties is a basic requirement for the successful use of these fibers. However, the main drawback of jute fiber is its hydrophilic nature that prevents it from having applications in high-end product.

Bamboo is a fast-growing species and a high-yield renewable resource in Borneo Island. The Asian and Oceanian regions are the highest producers of bamboo, with a combined 65% of the total bamboo resource worldwide. This region also includes 80% of the bamboo species in the world (Bystriakova *et al*. 2003; Chaowana 2013). Bamboo fibers have been widely used in the papermaking, textile, construction, and composite manufacturing industries. In addition, bamboo fibers possess many excellent properties, including high tensile, excellent thermal conductivity, and bacteria resistance. The fast-growing characteristics of bamboo is advantageous for its utilization (Chattopadhyay *et al*. 2011); however, bamboo has some limitations, such as low elasticity, high porosity, and poor wrinkle recovery when used in textiles (Liu and Hu 2008).

Hybrid composites are materials made from combining two or more different fibers in a common matrix. Hybrid composites can be produced from synthetic fibers, natural fibers, or a combination of both. Vijaya *et al*. (2015) confirmed that hybrid composites yield a better combination of properties than single fiber-reinforced composites (Vijaya *et al*. 2015). The constituent fibers in a hybrid composite can be altered in many ways, leading to variations in its properties. The mechanical properties, such as tensile strength, flexural strength, and impact strength, are maximal for jute and banana fiber-reinforced epoxy hybrid composites with a 1:1 ratio (Boopalan *et al*. 2013). Jawaid and Abdul Khalil (2011) investigated chemical and physical properties of hybrid palm oil fruit bunch-jute and found that hybrid empty fruit bunch-jute fiber composites showed improvement in physical properties compared to pure empty fruit bunch composites. John *et al*. (2008) studied the effect of chemical modification on the properties of sisal palm oil-reinforced composites. They found that the 4% NaOH-treated fiber resulted in the strongest mechanical properties with minimum fiber swelling.

The drawback of natural fibers is that they are naturally hydrophilic. Therefore, they are poorly compatible with hydrophobic matrixes. To overcome this, surface modification is needed to improve the hydrophilic property (Rahman *et al*. 2009). In this study, 4-methylcatechol in alkaline medium was used to treat jute and bamboo fibers to reduce the hydroxyl groups. In this present work, the effects of different pH treatments on the thermal, mechanical, and morphological properties of jute-bamboo hybrid fiber composites were investigated. Fabricated hybrid composites were characterized using thermogravimetric analysis, differential scanning calorimetry, and dynamic mechanical thermal analysis. Additionally, surface morphology, tensile testing and adhesion test was reported.

EXPERIMENTAL

Materials

Jute (*Corchorus olitorius*) and bamboo (*Dendrocalamus asper*) fibers were sourced from the Bangladesh Jute Research Institute (BJRI), Dhaka, Bangladesh, and the Forest Research Institute Sarawak, Malaysia, respectively. Low-density polyethylene (LDPE) resin was obtained from the Siam Polyethylene Co., Ltd., Prakanong, Bangkok, Thailand. The density was 0.935 gcm^{-3}, and the melting point ranged from 105 to 125 °C. 4-Methylcatechol (Sigma Aldrich, St. Louis, MO, USA), ethanol (Sigma Aldrich, St. Louis,

MO, USA), and sodium hydroxide (Merck KgaA, Darmstadt, Germany) were used in this study. All of the chemicals were of analytical grade.

Jute and Bamboo Fiber Preparation

The jute fibers were cleaned and air-dried for 48 h under direct sunlight. The middle portion of the jute fiber was removed and chopped into approximately 10-mm-long sections, and then oven-dried at 105 °C for 24 h. Finally, the sections were ground and sieved using a 100-µm sieve.

The length of the bamboo culm trim, excluding the bamboo internode, was 1 m in length. It was cut using a planer machine to chips, and then ground to powdered form. The chips and powder mixture were dried in an oven at 70 °C for 72 h. The oven-dried samples were grinded and sieved, using a 100-µm sieve, to obtain bamboo fibers with a mesh size of 100 µm.

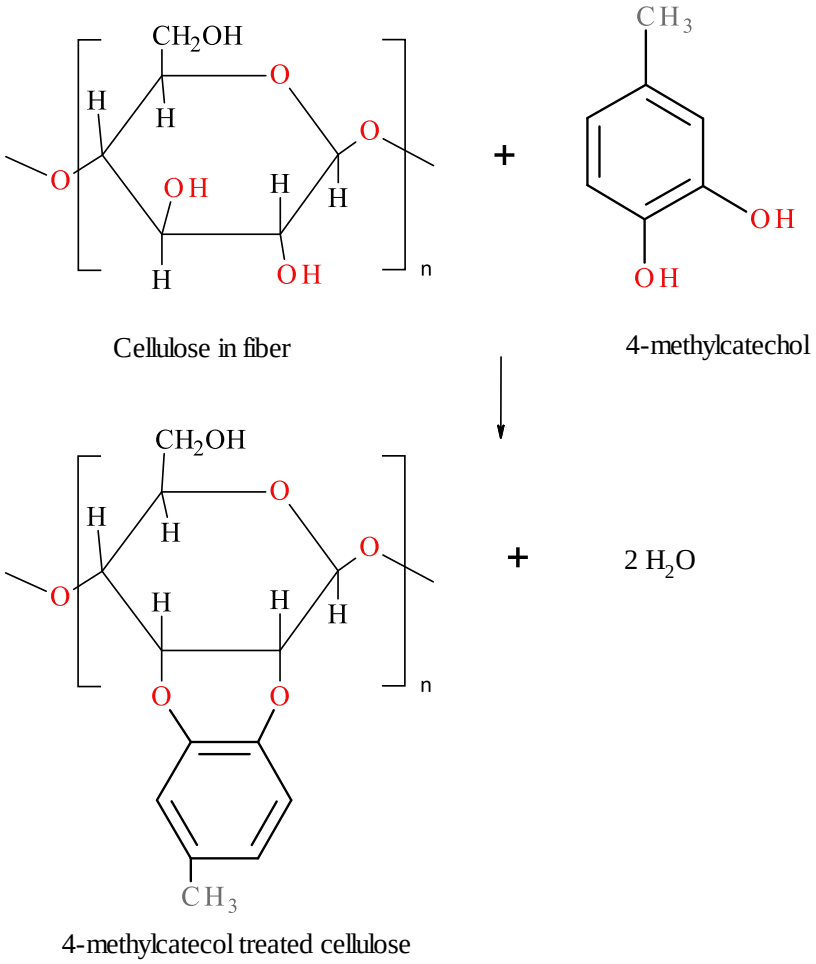

Fig. 1(a). The reaction scheme of jute and bamboo cellulose fiber with 4-methylcatechol

Chemical Treatment of Jute and Bamboo Fiber

Treatment solutions were prepared by dissolving 25 g of 4-methylcatechol in 500 mL of ethanol. Concentrated NaOH solution was added to maintain individual pH solutions of 7, 8, 9, and 10, respectively. Convection oven-dried jute and bamboo fibers were then immersed in the prepared pH solutions for 30 min. Subsequently, the treatment solution was filtered using filter paper. All of the remain fibers were rinsed three times using

deionized water and then air-dried in a convection oven at 100 °C for an additional 24 h. Treated jute and bamboo fibers were ground for 3 min and mixed at a weight ratio of 1:1 to obtain hybrid fibers. Figure 1(a) shows the reaction scheme of this surface treatment.

Composite Preparation

The hybrid fibers, treated at different pHs, were kept in a convection oven at 100 °C for 24 h prior to initiate composite fabrication. A 5% weight fraction of hybrid fiber was mixed thoroughly with a 95% weight fraction of LDPE granules to produce the hybrid fiber composite specimens. After obtaining the desired weight fraction, the mixture was poured into an aluminum mold for hot pressing at 190 °C with 3.45 MPa (500 psi) for 1 h. The prepared specimens were labeled F5pH*x*, where *x* corresponds to the pH level. The flow of hybrid composite fabrication is shown in Fig. 1 (b).

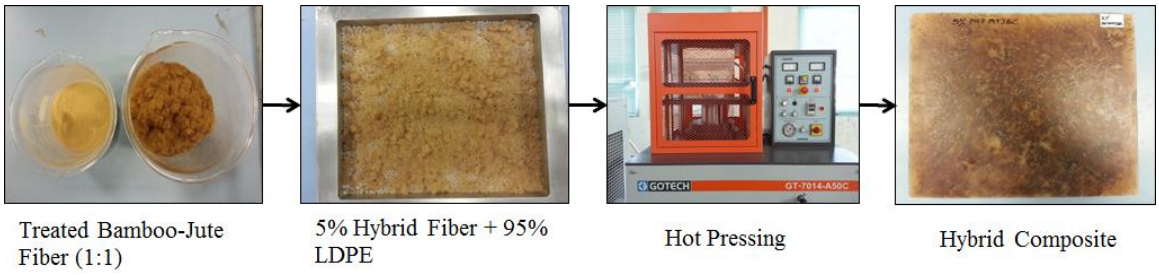

Fig. 1(b). The flow chart of hybrid composite fabrication

Characterization Methods

Fourier transform infrared spectroscopy (FTIR)

The FTIR spectra were obtained using a spectrometer (spectrum 100, Perkin Elmer, Waltham, MA). The obtained spectra are described in the results and discussion section. The transmittance range of the scan was 4000 to 650 cm^{-1}.

Thermogravimetric analysis (TGA)

Thermogravimetric measurements were performed using a Perkin Elmer Pyris 1 TGA system. All measurements were obtained under a nitrogen flow rate of 20 $mL \cdot min^{-1}$ over a temperature range of 50 to 600 °C. Then, an oxygen flow rate of 20 $mL \cdot min^{-1}$ and a temperature range of 600 to 700 °C was applied, while maintaining a constant heating rate of 20 $°C \cdot min^{-1}$.

Differential scanning calorimetry (DSC)

The DSC tests were conducted using a differential scanning calorimeter (DSC; 8000, Perkin Elmer). Temperature programs for dynamic tests were run from 50 to 180 °C at the heating rate of 20 $°C \cdot min^{-1}$ under a 20 $mL \cdot min^{-1}$ nitrogen atmosphere.

Dynamic mechanical thermal analysis (DMTA)

Dynamic mechanical thermal analysis was used to study the storage modulus (*E*') and loss tangent (tan δ) of the hybrid composites. Specimens with the dimensions, 30 mm × 10 mm × 3 mm, were tested using a single cantilever mode. The airflow atmosphere was 1 Hz and the heating rate was 2 $°C \cdot min^{-1}$. Measurements were obtained over a temperature range of 30 to 100 °C.

Tensile tests

Tensile testing was conducted according to the ASTM D 638-10 (2010) testing standard using a universal testing machine (MSC-5/500, Shimadzu Company Ltd., Japan) at a crosshead speed of 5 mm·min^{-1}. The dimensions of the specimens were 115 mm (*L*) × 6.5 mm (*W*) × 3.1 mm (*T*).

Scanning electron microscopy (SEM) analysis

The surface morphology was examined using a scanning electron microscope (TM 3030 pitch emission, Hitachi, Tokyo, Japan). The SEM specimens were sputter-coated with gold using auto fine coater (JFC-1600, Joel Ltd.)

Adhesion test

To evaluate the adhesion of the hybrid composite, a tape test was employed according to ASTM D 3359-09 (2009). Flatback Masking Tape (Scotch brand no. 250, 3M) with 25.4 mm width was used to conduct this test. A lattice pattern with six cuts in each direction was made on hybrid composites. The 20 mm long cuts were spaced 2 mm apart in each direction. A 75 mm long piece of the tester tape with center of tape was placed over the grid and rubbed firmly with an eraser on the end of a pencil. The tape was then removed by seizing the free end and pulling it off rapidly back upon itself at an angle 180^{o}. The adhesion was evaluated by comparison with description and illustration stated in the ASTM D3359 (2009). An evaluation scale (5B to 0B) is provided, where 5B is the best and 0B is the worst.

RESULTS AND DISCUSSIONS

Fourier Transform Infrared Spectroscopy

Figure 2 shows the untreated and treated jute fibers at various pH levels. The peak intensities with a transmittance band at approximately 3337 to 3347 cm^{-1} were assigned to O–H stretching vibrations, which gradually decreased after the 4-methylcatechol treatment. The decreasing intensity of the O–H bands indicated that the hydroxyl group content of the treated jute fibers was reduced (Rahman *et al*. 2011). The peak intensity at 2911 cm^{-1} was related to C-H stretching vibration, while the peak at 1643 cm^{-1} was attributed to H–O–H stretching vibration of absorbed water from carbohydrate. This peak was absent in the 4-methylcatechol-treated jute specimens at different pH levels. This indicates that the jute fiber after chemical treatment became more hydrophobic in comparison with the untreated fiber. The peak at 1738 cm^{-1} in Fig. 2 represents the obvious transmittance peak of lignin. The treated fibers, which had a lower peak, implied that lignin was only partially removed from jute fiber in the 4-methylcatecol pH control treatment.

Figure 3 shows the treated and untreated bamboo fibers at different pH levels. The peak intensity of the transmittance band at approximately 3338 cm^{-1} was assigned to the O–H stretching vibration, which drastically decreased after the 4-methylcatecol treatment. For the treated bamboo fiber, there was low intensity peak at 3338 cm^{-1}. The peak intensity at 1637 cm^{-1} was attributed to the H–O–H stretching vibration of absorbed water from carbohydrate of untreated fibers (Liew *et al*. 2015). The hydroxyl groups in all of the 4-methylcatecol-treated bamboo fibers were removed regardless of the pH level. This indicated that the bamboo fiber had become more hydrophobic compared to the untreated fiber after the chemical modification.

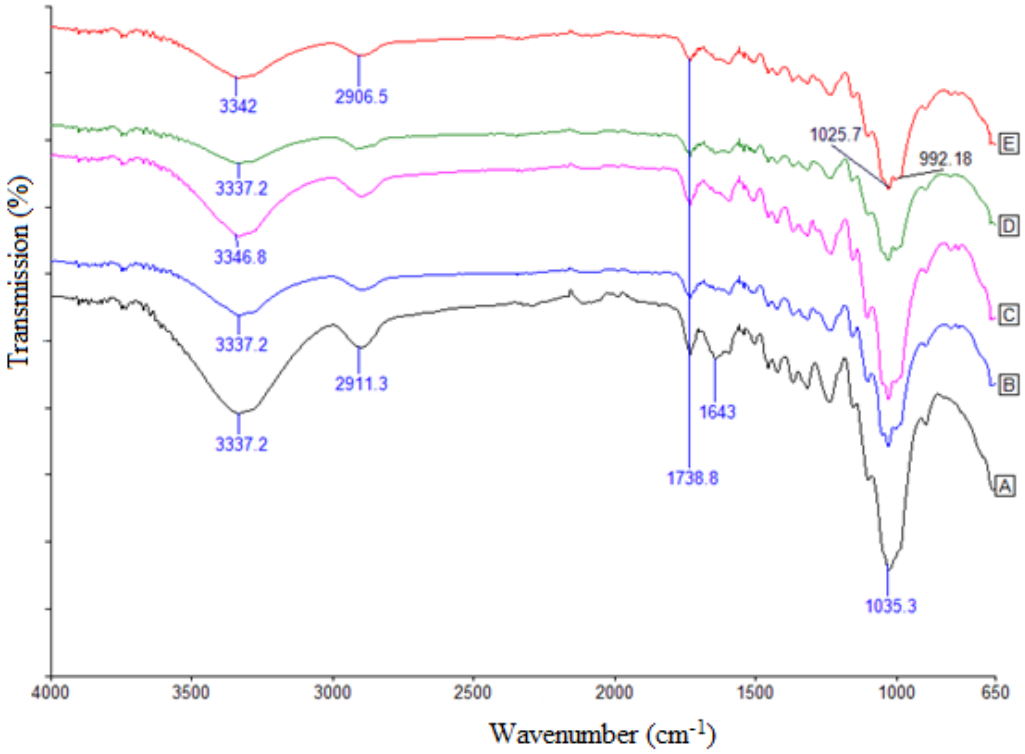

Fig. 2. Fourier transform infrared spectra of A) untreated and treated jute fiber at B) pH 7, C) pH 8, D) pH 9, and E) pH 10

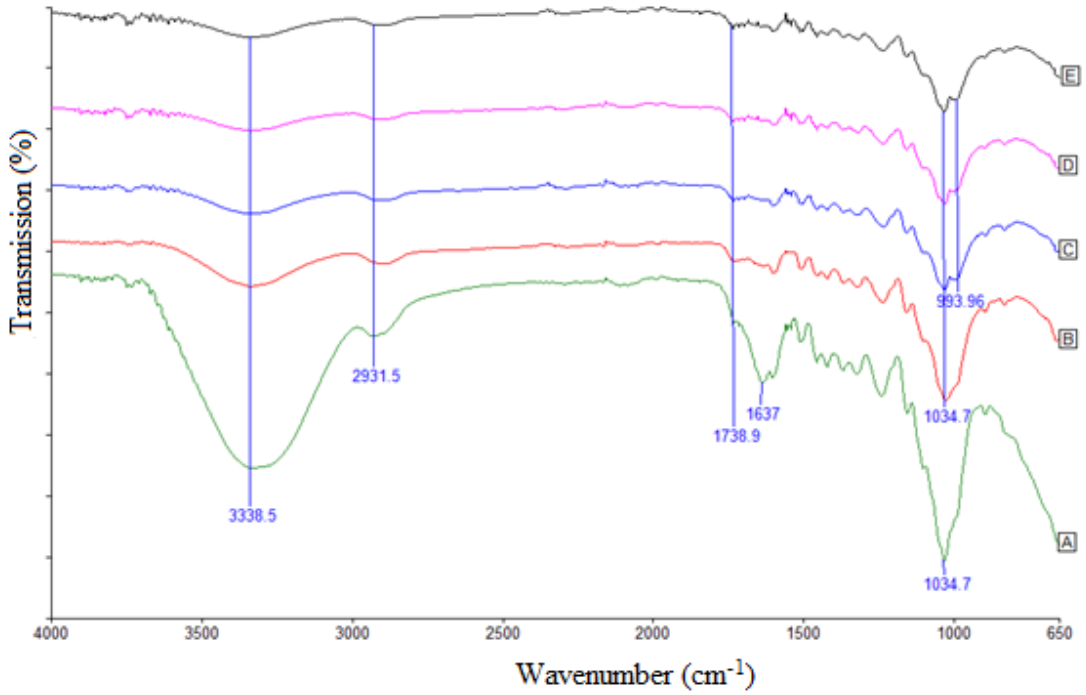

Fig. 3. Fourier transform infrared spectra of A) untreated and treated bamboo fiber at B) pH 7, C) pH 8, D) pH 9, and E) pH 10

A comparison of the treated jute and bamboo fibers indicated that higher pH (9 and 10) was effective for hydrophobic fibers modification in both fibers.

Thermogravimetric analysis (TGA)

The thermal stability of treated hybrid composites is shown in Fig. 4, which indicates that the decomposition of neat LDPE took place in the single step from 495 to 535 °C. Neat LDPE consisted of carbon–carbon bonds in the main chain that permitted a higher temperature which facilitated random scission at the weak sites of the main chain of the polymers.

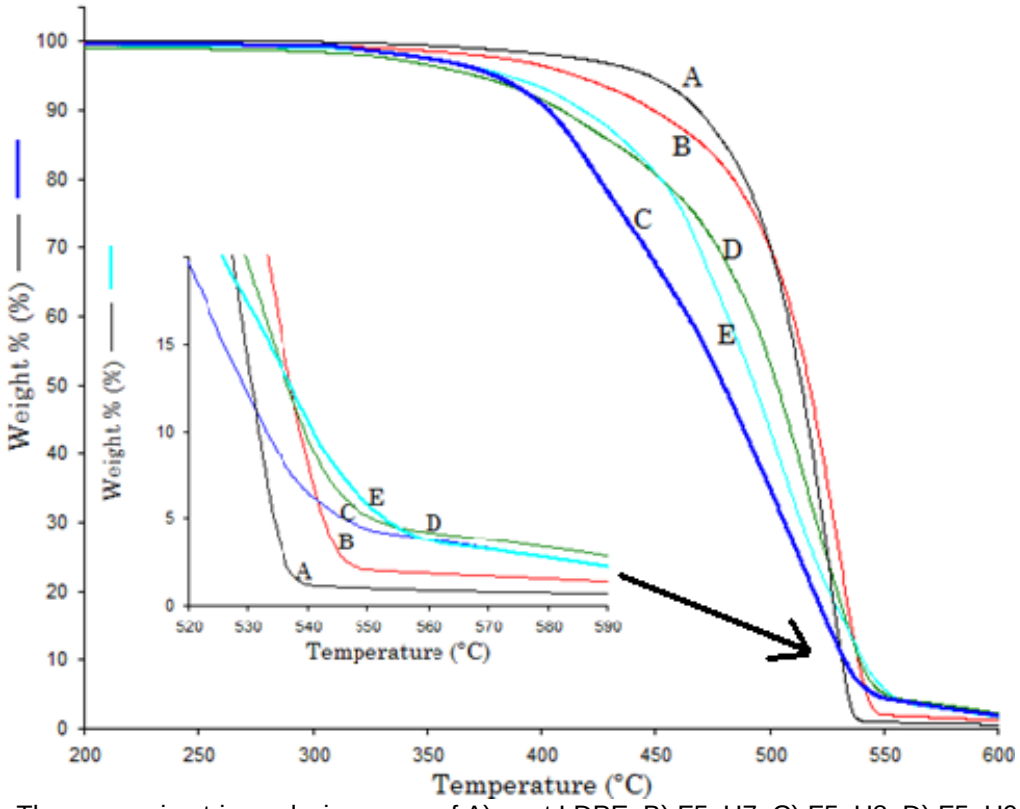

Fig. 4. Thermogravimetric analysis curves of A) neat LDPE, B) F5pH7, C) F5pH8, D) F5pH9, and E) F5pH10 hybrid composites

Table 1. Thermogravimetric Data for Low-Density Polyethylene (LDPE) and Hybrid Fiber Composites

Step no.	TG Data	LDPE	F5pH7	F5pH8	F5pH9	F5pH10
Step 1	T_i (°C)	-	402.2	384.7	366.3	385.3
	T_m (°C)	-	446.9	420.8	419.6	437.4
	T_f (°C)	-	503.3	471.2	480.8	464.8
	W_i (wt.%)	-	19.9	42.7	24.5	22.8
Step 2	T_i (°C)	495.3	503.3	471.2	480.8	464.8
	T_m (°C)	528.0	532.3	518.9	516.7	510.6
	T_f (°C)	535.1	542.1	541.1	543.6	543.8
	W_i (wt.%)	98.5	76.1	52.3	69.6	72.2
	Residual (%)	1.5	4.0	5.0	5.9	5.0

T_i: onset temperature; T_m: temperature corresponding to the maximum rate of mass loss; T_f: end temperature; W: mass loss; TG: Thermogravimetric

On the other hand, the decomposition process of hybrid fiber composites took place in two steps. For F5pH7, there was a mass loss of 20 wt.% from hybrid fibers that took place at 402 to 503 °C and 76 wt.% from the LDPE matrix that took place at 503 to 542 °C. The final residues were detected at 4 wt.%. The reduction in decomposition temperature could be explained by the lower thermal degradation temperature of the cellulose in fibers than of the neat LDPE (Sdrobiş *et al*. 2012). It was confirmed that the thermal stability (maximum decomposition of fiber-matrix) of the F5pH7 hybrid fiber composites was higher than the neat LDPE, as shown in Table 1. The present finding is supported by previous findings which indicate that the addition of fibers improved the thermal resistance of composites (Averous and Boquillon 2004).

However, the hybrid fiber composites treated at pH 8, 9, and10 degraded at lower temperatures than the neat LDPE. This indicates that the presence of hybrid fiber treated at higher pH led to earlier degradation than the neat LDPE. The increase of pH not only led to a reduction of 6 to 17 °C of peak decomposing temperature but extended the final temperature by 6 to 8 °C. In addition, the char residue of the hybrid composites was larger than that of the neat LDPE (Table 1). Moreover, there was no significant weight loss below a temperature of 300 °C, which was 57.8% higher than the processing temperature of LDPE composites. Therefore, it could be concluded that there was no thermal degradation occurring in the hybrid composites that were processed at 190 °C.

Differential scanning calorimetry

Differential scanning calorimeter was used to determine thermal stability. It measures the heat capacity of the sample, glass transition temperature (T_g), and melting point temperature (T_m). The characteristic temperatures of the crystallization peaks are summarized in Fig. 5.

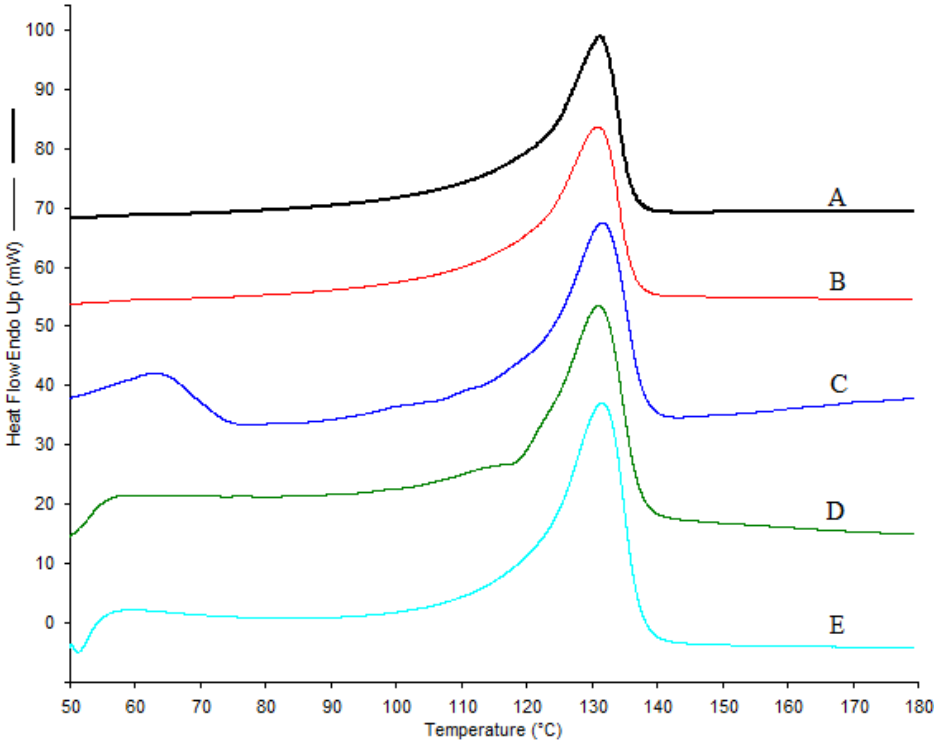

Fig. 5. Differential scanning calorimetry thermograms for thermal analysis of A) neat Low density polyethene, B) F5pH7, C) F5pH8, D) F5pH9, and E) F5pH10

Table 2. Melting Characteristics of Hybrid Fibers Composites:

Specimen	Initial melting temperature (°C)	Final melting temperature (°C)	Peak melting temperature (°C)	Heat flow ΔH_m (Jg^{-1})	Crystallinity (X_c)
Neat LDPE	119.44	136.08	131.30	162.10	0.559
F5pH7	118.83	136.24	130.94	133.48	0.485
F5pH8	121.74	137.33	131.49	132.72	0.482
F5pH9	119.70	136.79	131.13	134.35	0.488
F5pH10	119.96	137.20	131.52	130.78	0.475

In Table 2, ΔH_m is the enthalpy of fusion, X_c is the degree of crystallinity,

$$X_c = \frac{\Delta H_m}{w\Delta H_m^o} \quad (1)$$

and w are the weight fractions of polymeric matrix in the composite, and ΔH_m^o =290 J/g (heat of fusion for 100% crystalline LDPE).

According to the results (Table 2), the peak melting temperature of the matrix was not influenced by the addition of hybrid fiber under various pH treatments. However, the crystallinity index was drastically reduced from 55.9 to between 47.5 and 48.8 with increasing the pH of the hybrid fiber treatment. A drop of 7% to 8% in the crystallinity index by the addition of 5 wt.% hybrid fiber can be related to a change in the crystallinity behavior of LDPE in the presence of hybrid fiber. Hydrogen bond formation occurring between the fibers-matrix reduces the crystallinity index of the hybrid composite (Kumar *et al*. 2010). A reduction in the crystallinity index was an indicator of an improvement in the adhesion between the fiber and the polymeric matrixes.

Dynamic mechanical thermal analysis (DMTA)

The viscoelastic behavior of hybrid composites was studied using DMTA. The storage/elastic modulus (E') and the loss tangent (tan δ) are shown in Figs. 6 and 7, respectively. Figure 6 shows the decrease in the storage modulus with increasing temperature because of the dilute nature of the polymer at all of the pH conditions (Rajini *et al*. 2013). It was clearly shown that the highest storage modulus (E') was obtained for F5pH10 at room temperature. A high storage modulus indicates that there is a strong interfacial bonding relationship between the high pH-treated hybrid fibers and the matrix (Hamdan *et al*. 2010). Because of this relationship, the high pH-treated fibers prevented free molecular motion of the composite to an extent (Pothan *et al*. 2010).

The variation in the damping parameter (tan δ) was shown in Fig. 7. This property indicates that efficient materials loose energy to molecular rearrangements and internal friction. The tan δ value of the treated hybrid fiber composites was higher compared to neat LDPE, except for F5pH7 and F5pH10 at low temperature (< 65 °C). At room temperature, the tan δ value of F5PH10 was the lowest among the composites. A lower tan δ implies a higher elastic recovery. Therefore, F5pH10 exhibited strong interactions between the fibers and the matrix, which tended to reduce the mobility of the molecular chains at the interface, subsequently reducing the damping.

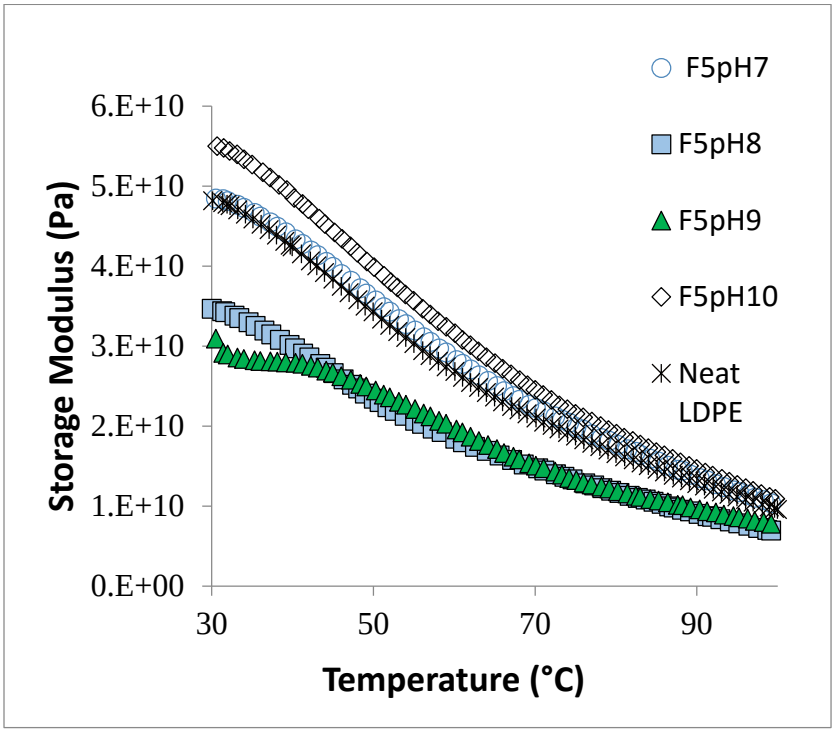

Fig. 6. Storage modulus of different pH-treated hybrid fiber composite according to temperature

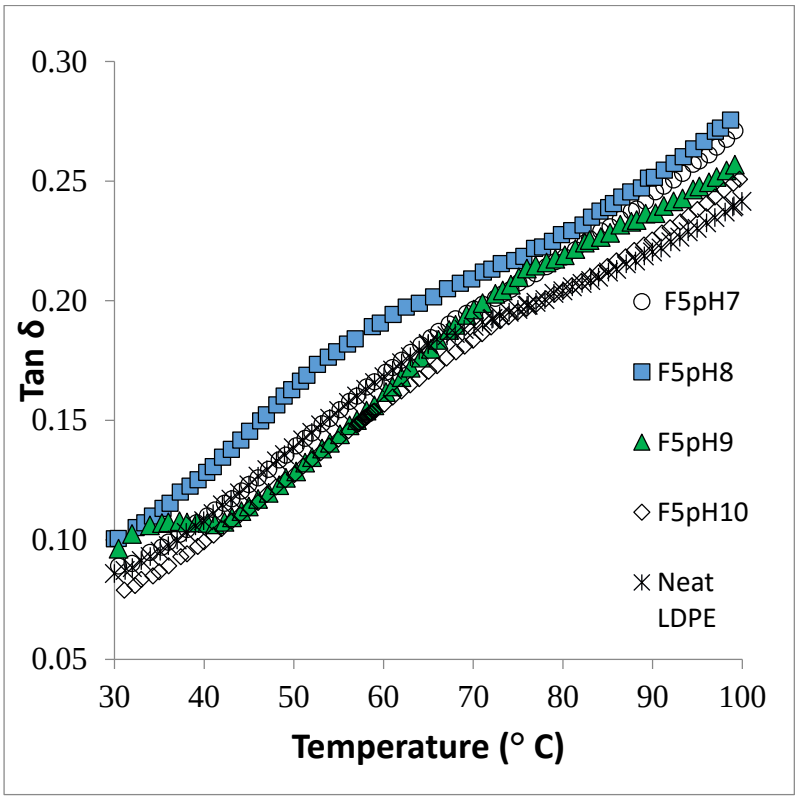

Fig. 7. Loss tangent of different pH-treated hybrid fiber composite according to temperature

However, at high temperatures all specimens had an increasing trend for damping. At temperatures below 70 °C, F5pH10 performed well, with the lowest in damping. F5pH7 showed a similar trend with damping behavior as compared with neat LDPE at temperatures below 65 °C. All specimens exhibited high damping behavior at or above 70 °C. F5pH8 showed the highest damping behavior from room temperature to 100 °C. The TGA result also revealed that the F5pH8 treated hybrid fiber composite had the greatest degree of decomposition at an early stage. All those results implied relative weak bonding between the fiber and matrix from F5pH8.

Tensile properties

The tensile strength (TS) and Young modulus (*E*) of the different pH-treated hybrid fiber composite are shown in Figs. 8 and 9. It was observed that the TS and *E* did not increase linearly with pH. Among the hybrid composites, F5pH7 and F5pH10 showed the greatest improvement in TS and *E*, compared with neat LDPE. The F5PH7 composite revealed a 7% and 23% increase in TS and *E*, respectively. The F5pH10 composite showed notable improvements in TS and E of 16% and 37%, respectively. The TS and E of F5pH10 revealed that the stress was more evenly distributed and was optimized. The increase in elastic modulus indicated that a stress transfer ensured by the treated hybrid fibers (Bledzki and Jaszkiewicz *et al*. 2010).

Thus, fiber treatment at higher pH was able to improve the fiber matrix interfacial adhesion capability, leading to better stress transfer efficiency from the matrix to the fiber, and consequently the treatment improved the composite's mechanical properties (Hossen *et al*. 2015).

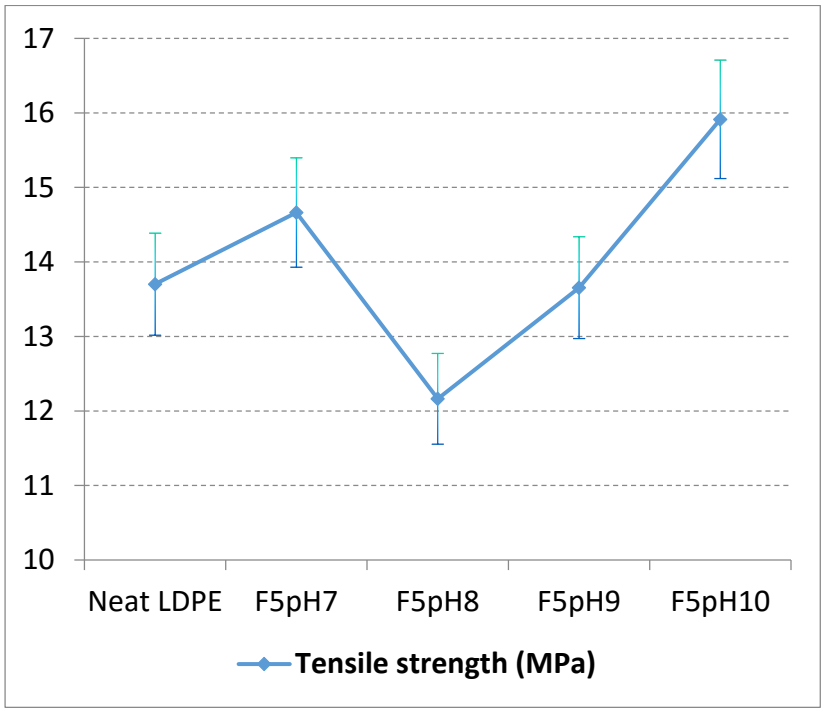

Fig. 8. Tensile strength for different pH-treated hybrid fiber composites

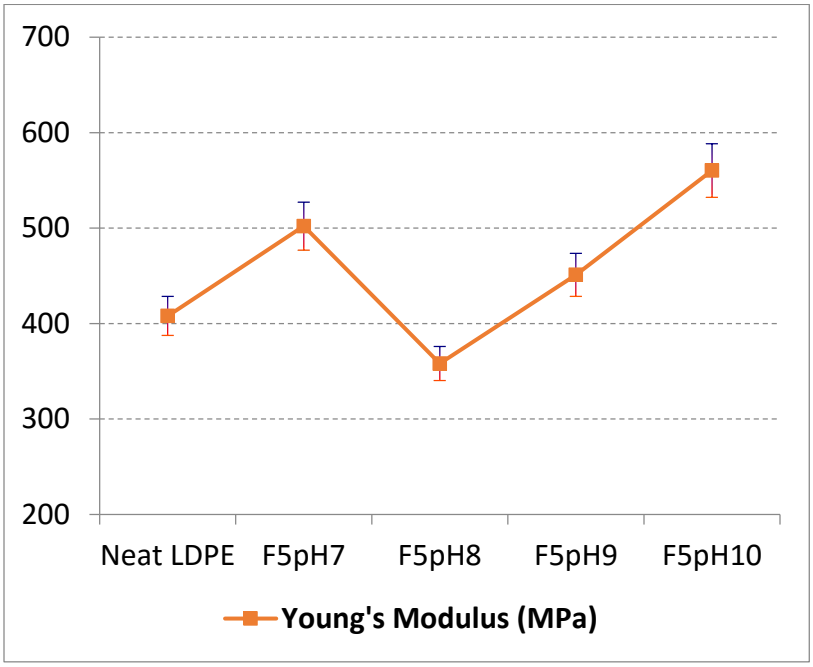

Fig. 9. Young's modulus for different pH-treated hybrid fiber composites

Scanning electron microscopy analysis

Scanning electron microscopy was used to investigate the surface morphology of the fractured specimen of F5pH7, F5pH8, F5pH9, and F5pH10 (Fig. 10). A considerable difference was found among the hybrid fiber composites because of the differences in interfacial bonding between the treated fibers and the matrix.

Figure 10a shows a well bonded interface between the hybrid fiber and the matrix of F5pH7. The fibers were strongly held by the LDPE, which flowed smoothly during the hot pressing process. This strong interfacial bond between the treated hybrid fibers and the LDPE matrix contributed to a higher tensile strength and modulus. This strong interfacial bonding was attributed to a reduction in the hydroxyl groups from chemical surface modification of hybrid fibers by 4-methylcatecol at pH 7 (Rahman *et al.* 2015). Figure 10b clearly shows the weak bonding of F5pH8. There were some voids because of the relatively weak interfacial bonding between the fibers and the matrix. Weak adhesion between the fibers and the matrix creates voids in the composite. Figure 10c shows the bonded interface between the hybrid fiber and matrix, with some traces of treated bamboo fibers found on the matrix surface.

The interfacial bonding between the treated jute fiber and the LDPE matrix contributed to good tensile strength and modulus. The interfacial bonding of F5pH9 was weaker than F5pH7 because some of the treated bamboo fibers were loose and weak in the interfacial adhesion. Figure 10d shows good adhesion between the treated hybrid fibers and the LDPE matrix. The treated hybrid fibers in a strong alkaline environment (pH 10) showed high tensile strength and Young's modulus (F5pH10). The hydrophobic characteristics of treated hybrid fibers enhance the fibers-matrix interfacial adhesion (Islam *et al.* 2010). Scanning electron microscopy revealed that the treated fibers buried in smooth flow LDPE resin were not pulled out and no voids were found on those matrix surface areas.

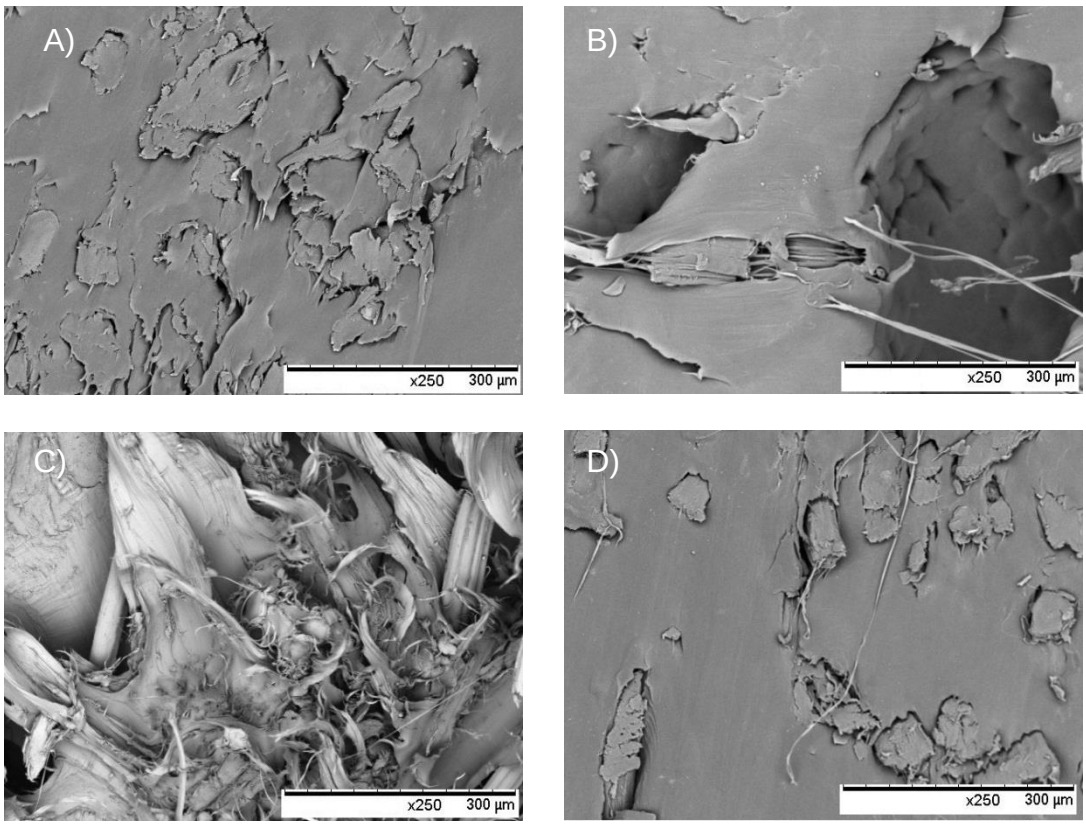

Fig. 10. Scanning electron micrograph images of the cross sectional surface area of A) F5pH7 B) F5pH8 C) F5pH9, and D) F5pH10

Adhesion Test

The adhesion test results are shown in Table 3. According to the finding, there was no fiber peel off for F5pH7 and F5pH10, respectively. On the other hand, 8% and 4% fiber peel off were observed in F5pH8 and F5pH9 (Grove *et al*.1999). It indicated that F5pH8 and F5pH9 showed low adhesion compare to F5pH7 and F5pH10 which reflect in SEM results.

Table 3. Analysis of Adhesion Tests of Hybrid Fibers Composites

No	Samples	Evaluation Results	Remark
1	F5pH7	5B 0% None	None peel off observe
2	F5pH8	3B 5-15%	8% peel off observe
3	F5pH9	4B Less than 5%	4% peel off observe
4	F5pH10	5B 0% None	None peel off observe

CONCLUSIONS

1. The results clearly showed that the 4-methylcatechol solution, at high pH, successfully produced hydrophobic bamboo and jute fibers. Both treated fibers showed that the OH group was significantly reduced from the cellulose molecule.
2. The introduction of treated hybrid fibers lowered the decomposition temperature. High pH-treated hybrid composites exhibited a significant reduction in the peak decomposition temperature and an extension of the final temperature.
3. Dynamic mechanical thermal analysis showed that the high pH-treated hybrid fiber composite exhibited an improvement in the high storage modulus and low loss tangent.
4. Higher pH-treated hybrid fiber composites exhibited good interfacial bonding between fibers and the matrix. This contributed to the highest tensile strength and Young's modulus.
5. The increment of pH level in the fiber treatment improved the hydrophobicity of the fibers.

ACKNOWLEDGMENTS

The authors would like to acknowledge the center of excellence and renewable energy (CoERE), and UNIMAS for their financial support, Grant No. CoERE/Grant/2013/06.

REFERENCES CITED

ASTM D3359 (2009). "Standard Test Methods for Measuring Adhesion by Tape Test, ASTM International, West Conshohocken, PA.

ASTM D 638 (2010). "Standard Test Method for Tensile Properties of Plastics," ASTM International, West Conshohocken, PA.

Averous, L., and Boquillon, N. (2004). "Biocomposites based on plasticized starch: Thermal and mechanical behaviours," *Carbohydrate Polymers* 56(2), 111-122. DOI: 10.1016/j.carbpol.2003.11.015

Botelho, E. C., Silva, R. A., Pardini, L. C., and Rezende, M. C. (2006). "A review on the development and properties of continuous fiber/epoxy/aluminum hybrid composites for aircraft structures," *Materials Research* 9(3), 247-256. DOI: 10.1590/S1516-14392006000300002

Boopalan, M., Niranjanaa, M., and Umapathy, M. J. (2013). "Study on the mechanical properties and thermal properties of jute and banana fiber reinforced epoxy hybrid composites," *Composites Part B: Engineering* 51, 54-57. DOI: 10.1016/j.compositesb.2013.02.033

Bledzki, A., and Jaszkiewicz, A. (2010). "Mechanical performance of biocomposites based on PLA and PHBV reinforced with natural fibres – A comparative study to PP," *Composites Science and Technology* 70(12), 1687-1696. DOI: 10.1016/j.compscitech.2010.06.005

Bystriakova, N., Kapos, V., Lysenko, I., and Stapleton, C. M. A. (2003). "Distribution and conservation status of forest bamboo biodiversity in the Asia-Pacific Region," *Biodiversity and Conservation* 12(9), 1833-1841. DOI: 10.1023/A:1024139813651

Chaowana, P. (2013). "Bamboo: An alternative raw material for wood and wood-based composites," *Journal of Materials Science Research* 2(2), 90. DOI: 10.5539/jmsr.v2n2p90

Chattopadhyay, S. K., Khandal, R. K., Uppaluri, R., and Ghoshal, A. K. (2011). "Bamboo fiber reinforced polypropylene composites and their mechanical, thermal, and morphological properties," *Journal of Applied Polymer Science* 119(3), 1619-1626. DOI: 10.1002/app.32826

Grove, N. R., Kohl, P. A., Bidstrup Allen, S. A., Jayaraman, S., and Shick, R. (1999). "Functionalized polynorbornene dielectric polymers: Adhesion and mechanical properties," *Journal of Polymer Science Part B Polymer Physics* 37(21), 3003-3010. DOI: 10.1002/(SICI)1099-0488(19991101)37:21<3003::AID-POLB10>3.0.CO;2-T

Hamdan, S., Rahman, M. R., Ahmed, A. S., Talib, Z. A., and Islam, M. S. (2010). "Influence of N, N-dimethylacetamid on the thermal and mechanical properties of polymer-filled wood," *BioResources* 5(4), 2611-2624. DOI: 10.15376/biores.5.4.2611-2624

Hitoshi, T., Norio, N. A., and Ke, L. (2014). "Effect of microstructure on multifunctional properties of natural fiber composites," *Blucher Material Science Proceedings* 1(1), 62-65. DOI: 10.5151/matsci-mmfgm-091-f

Hossen, M. F., Hamdan, S., Rahman, M. R., Rahman, M. M., Liew, F. K., and Lai, J. C. (2015). "Effect of fiber treatment and nanoclay on the tensile properties of jute fiber reinforced polyethylene/clay nanocomposites," *Fibers and Polymers* 16(2), 479-485. DOI: 10.1007/s12221-015-0479-x

Islam, M. N., Rahman, M. R., Haque, M. M., and Huque, M. M. (2010). "Physico-mechanical properties of chemically treated coir reinforced polypropylene composites," *Composites Part A: Applied Science and Manufacturing* 41(2), 192-198. DOI: 10.1016/j.compositesa.2009.10.006

Jahan, M. S., Gunter, B. G., and Rahman, A. (2009). "Substituting wood with nonwood fibers in papermaking: A win-win solution for Bangladesh," BDRWPS *Working paper No. 4*, DOI : 10.2139/ssrn.1322292

Jawaid, M., and Abdul Khalil, H. (2011). "Cellulosic/synthetic fibre reinforced polymer hybrid composites: A review," *Carbohydrate Polymers* 86(1), 1-18. DOI: 10.1016/j.carbpol.2011.04.043

John, M. J., Francis, B., Varughese, K., and Thomas, S. (2008). "Effect of chemical modification on properties of hybrid fiber biocomposites," *Composites Part A: Applied Science and Manufacturing* 39(2), 352-363. DOI: 10.1016/j.compositesa.2007.10.002

Joshi, S. V., Drzal, L., Mohanty, A., and Arora, S. (2004). "Are natural fiber composites environmentally superior to glass fiber reinforced composites?" *Composites Part A: Applied Science and Manufacturing* 35(3), 371-376. DOI: 10.1016/j.compositesa.2003.09.016

Kim, K. Y., and Ye, L. (2012). "Interlaminar fracture properties of weft-knitted/woven fabric interply hybrid composite materials," *Journal of Materials Science* 47(20), 7280-7290. DOI: 10.1007/s10853-012-6682-x

Kumar, S., Choudhary, V., and Kumar, R. (2010). "Study on the compatibility of unbleached and bleached bamboo-fiber with LLDPE matrix," *Journal of Thermal Analysis and Calorimetry* 102(2), 751-761. DOI: 10.1007/s10973-010-0799-4

Lee, S. H., Wang, S., and Terarnot, Y. (2008). "Isothermal crystallization behavior of hybrid biocomposite consisting of regenerated cellulose fiber, clay, and poly(lactic acid)," *Journal of Applied Polymer Science* 108(2), 870-875. DOI: 10.1002/app.26853

Liew, F. K., Hamdan, S., Rahman, M. R., Rusop, M., Lai, J. C. H., Hossen, M. F., and Rahman, M. M. (2015). "Synthesis and characterization of cellulose from green bamboo by chemical treatment with mechanical process," *Journal of Chemistry* 2015, 212158. DOI: 10.1155/2015/212158

Liu, Y., and Hu, H. (2008). "X-ray diffraction study of bamboo fibers treated with NaOH," *Fibers and Polymers* 9(6), 735-739. DOI: 10.1007/s12221-008-0115-0

Nunna, S., Chandra, P. R., Shrivastava, S., and Jalan, A. (2012). "A review on mechanical behavior of natural fiber based hybrid composites," *Journal of Reinforced Plastics and Composites* 31(11), 759-769. DOI: 10.1177/0731684412444325

Pothan, L. A., George, C. N., John, M. J., and Thomas, S. (2010). "Dynamic mechanical and dielectric behavior of banana-glass hybrid fiber reinforced polyester composites," *Journal of Reinforced Plastics and Composites* 29(8), 1131-1145. DOI: 10.1177/0731684409103075

Rajini, N., Jappes, J. W., Rajakarunakaran, S., and Jeyaraj, P. (2013). "Dynamic mechanical analysis and free vibration behavior in chemical modifications of coconut sheath/nano-clay reinforced hybrid polyester composite," *Journal of Composite Materials* 47(24), 3105-3121. DOI: 10.1177/0021998312462618

Rahman, R., Hasan, M., Huque, M., and Islam, N. (2009). "Physico-mechanical properties of maleic acid post treated jute fiber reinforced polypropylene composites," *Journal of Thermoplastic Composite Materials* 22(4), 365-381. DOI: 10.1177/0892705709100664

Rahman, M., Hamdan, S., Ahmed, A. S., Islam, M., Talib, Z. A., Abdullah, W., and Mat, M. (2011). "Thermogravimetric analysis and dynamic Young's modulus measurement of N, N-dimethylacetamide-impregnated wood polymer composites," *Journal of Vinyl and Additive Technology* 17(3), 177-183. DOI: 10.1002/vnl.20275

Rahman, M. R., Hamdan, S., Hasan, M., Baini, R., and Salleh, A. A. (2015). "Physical, mechanical, and thermal properties of wood flour reinforced maleic anhydride grafted unsaturated polyester (UP) biocomposites," *BioResources* 10(3), 4557-4568. DOI :10.15376/biores.10.3.4557-4568

Article submitted: April 10, 2016; Peer review completed: June 5, 2016; Revised version received and accepted: June 16, 2016; Published: July 6, 2016.
DOI: 10.15376/biores.11.3.6880-6895